

**UC Berkeley**  
**SEMM Reports Series**

**Title**

A Theoretical and Experimental Study of Projectile Impact on Clamped Circular Plates

**Permalink**

<https://escholarship.org/uc/item/4x04g591>

**Authors**

Kelly, James

Wilshaw, T. R.

**Publication Date**

1967-09-01

REPORT NO. 67-26

STRUCTURES AND MATERIALS RESEARCH  
DEPARTMENT OF CIVIL ENGINEERING

---

---

# A THEORETICAL AND EXPERIMENTAL STUDY OF PROJECTILE IMPACT ON CLAMPED CIRCULAR PLATES

by  
J. M. KELLY  
and  
T. R. WILSHAW

Interim Technical Report  
National Science Foundation  
Grant No. GK-1065

---

---

SEPTEMBER, 1967

STRUCTURAL ENGINEERING LABORATORY  
UNIVERSITY OF CALIFORNIA  
BERKELEY CALIFORNIA

A Theoretical and Experimental Study  
of  
PROJECTILE IMPACT ON CLAMPED CIRCULAR PLATES

by

James M. Kelly

Division of Structural Engineering

and Structural Mechanics

Department of Civil Engineering

University of California

Berkeley

and

T. R. Wilshaw

Department of Materials Science

Stanford University

### Abstract

A method for the analysis of the plastic deformation of a circular plate subject to projectile impact is presented based on the assumption that the material is rigid viscoplastic, obeying a von Mises yield condition and associated flow rule. The predictions of the analysis are compared with the results of experiments in which projectiles of different masses are fired at various velocities at clamped plates of mild steel. The plates used in the experiments are such that substantial plastic strains can develop while the maximum displacements are of the same order as the thickness. The analytical method presented predicts the behavior of the plates to within the accuracy of the tests. The material constants which fit the results are in accord with those obtained from different tests.

## I. Introduction

One of the more interesting problems of structural mechanics is the analysis of the behavior of structural systems which are subject to impulsive loading and there are increasing demands for the design of structural systems which will withstand high stresses and often substantial plastic deformations for very short periods of time. In general a complete description of the history of stress and strain could only be obtained by massive and expensive computation and even if available there are problems of interpretation, and some question as to the applicability of material properties obtained from conventional tests to such situations. There exists therefore a two fold need. On the one hand a rapid method is needed for the prediction of the major features of the dynamic structural response in the plastic range, and on the other hand an experimental method is needed for obtaining relevant data which cannot be obtained by conventional tests.

In this paper we are concerned with the dynamic plastic behavior of a particularly simple structural system namely a clamped circular plate subject to impact by a cylindrical projectile. We will demonstrate the application of a particular method of analysis showing how the method predicts the overall behavior of the system in good agreement with experimental results which are also reported here. Further, we will show that the experimental model provides a simple method for the determination of the dynamic biaxial plastic behavior of a material at strain rates of the order of  $100-300 \text{ sec}^{-1}$ , this being intermediate between the pseudo-static biaxial test method of Lindholm and Yeakley [1] for strain rates below  $10 \text{ sec}^{-1}$  and

the higher strain rates of stress wave methods which are however uniaxial stress (see for example [2]) or uniaxial strain (for example [3]).

The problem of the dynamic deformation of a thin plate on the basis of rigid perfectly plastic rate independent material behavior has been studied by a number of authors. The responses of a simply supported plate to an ideal impulse and a rectangular pulse were examined by Wang [4] and by Hopkins and Prager [5] respectively. Recently Florence has obtained the response of a clamped plate to a rectangular pulse over the entire surface [6] and over a central region [7]. In all of the above cases a Tresca yield condition was assumed.

Experimental studies corresponding to the above theoretical analyses provide results which are considerably different from the theoretical predictions (see for example [8]); the differences have generally been attributed to the effects of membrane forces which are neglected in the analyses. However all these solutions were based on the assumption that the yield stress of the material was independent of strain rate, but the plastic behavior of mild steel, the most commonly used structural material, is very sensitive to strain rate. Furthermore the flow rule associated with the Tresca yield condition leads to velocity fields which are unrealistic as a result of the piecewise constant direction required of the strain rate vector. It is possible then that some of the discrepancies between theory and experiment might be eliminated by inclusion of rate effects and the use of a von Mises yield condition.

In the present paper the behavior of the plate is analyzed

on the basis of a rigid viscoplastic material obeying the von Mises yield condition and associated flow rule. The system of equations resulting from this material assumption is non-linear but a method of linearization used by Wierzbicki [9] in a problem of impulsive loading over the entire surface of a plate can be used also for the plate subject to projectile impact [10]. In this solution the effects of changes in geometry and membrane action are neglected but as the displacements of the plates in the experiments rarely exceed the plate thickness this is not an unrealistic assumption.

The closed form solution given here is similar to that given in [10] but has wider application. An approximation to the closed form solution was developed in [10] but is valid only for projectiles which are massive in comparison to the plate. In this case the projectiles are quite light in comparison to the plate and for such cases a different approximation has been developed.

## II. Theoretical Considerations

### (i) Visco-plastic Stress Strain Relations

The uniaxial stress strain behavior of mild steel at high strain rates has been studied for many years and it is generally recognized to be very rate sensitive. For example, the material used in the tests described in this paper has a static yield strength in simple tension of 35,000 psi (at a strain rate of  $10^{-3}$   $\text{sec}^{-1}$ ) and a yield strength of 58,000 psi at a strain rate of  $3 \times 10^2$   $\text{sec}^{-1}$ . The uniaxial behavior may be approximately represented by a linear relationship between stress  $\sigma$  and plastic strain rate  $\dot{\epsilon}$  of the form

$$\dot{\epsilon} = \frac{2}{\sqrt{3}\tau} (\sigma - \sigma_0) / \sigma_0 \quad (1)$$

where  $\sigma_0$  is the static yield stress in simple tension and  $\tau$  is the viscoplastic relaxation time of the material which for the above values of  $\sigma, \sigma_0$  and  $\dot{\epsilon}$  is 2.5 msec.

Generalizations of Equation (1) to non-uniaxial stress have been considered by a number of authors; in particular Perzyna [11] and Craggs [12] from different basic premises have obtained several forms of multiaxial stress strain relation. The simplest form which reduces to Equation (1) for uniaxial loading, and which will be used here is

$$\dot{\epsilon}_{ij} = \frac{1}{\tau} \frac{(s_{kl}s_{kl}/2)^{1/2-k}}{k} \cdot \frac{s_{ij}}{(s_{kl}s_{kl}/2)^{1/2}} \quad (2)$$

applicable when  $1/2 s_{kl}s_{kl} \geq k^2$ . In Equation (2)  $\dot{\epsilon}_{ij}$  is the strain rate tensor and  $s_{ij}$  the stress deviator,  $\tau$  is as before the relaxation time and  $k = \sigma_0 / \sqrt{3}$  the static yield stress in simple shear. The material is taken as incompressible for plastic deformations



and the elastic deformations are neglected.

The physical basis of Equation (2) is the assumption that the material obeys the von Mises criterion

$$1/2 s_{ij}s_{ij} = k^2$$

and its associated flow rule for static deformations and an expanded von Mises yield condition and associated flow rule for dynamic deformations, and further the viscosity of the material requires that the strain rate depend on the difference between the expanded and the static yield condition. The expansion of the yield condition at any time and any location in the body is given by squaring both sides of Equation (2) leading to

$$(1/2s_{ij}s_{ij})^{1/2} = k[1+\tau(1/2\varepsilon_{ij}\varepsilon_{ij})^{1/2}] \quad (3)$$

The flow rule asserts that the strain rate should be normal to the yield surface at any time. In the nine-dimensional space of the stress deviator the yield condition is a hypersphere and the requirement of the flow rule is met by noting that  $s_{ij}/(s_{kl}s_{kl})^{1/2}$  is a radial unit vector in this space.

#### (ii) Governing Equations of Thin Plate Theory

In setting up the governing equations of the viscoplastic plate all quantities are assumed to be functions only of  $r$  the distance measured from the plate center and of the time  $t$ . The surface tractions  $p$  or  $p_0$  are taken positive in the direction of positive transverse displacements of the middle surface. The velocity of points of the middle surface is  $v(r,t)$ . The plate radius is  $R$ , the thickness is  $2h$  and the mass density per unit of area of the

plate middle surface is  $\mu$  .

The constitutive relations of Equation (2) when written in terms of the radial and circumferential moments  $M_r$  and  $M_\phi$  and the corresponding curvature rates  $\kappa_r$  and  $\kappa_\phi$  take the form (see for example [13])

$$\left. \begin{aligned} \kappa_r &= \frac{\sqrt{3}}{2h\tau} \left( 1 - \frac{M_o}{\sqrt{M_r^2 - M_r M_\phi + M_\phi^2}} \right) \frac{2M_r - M_\phi}{M_o} \\ \kappa_\phi &= \frac{\sqrt{3}}{2h\tau} \left( 1 - \frac{M_o}{\sqrt{M_r^2 - M_r M_\phi + M_\phi^2}} \right) \frac{2M_\phi - M_r}{M_o} \end{aligned} \right\} (4)$$

where  $M_o = \sigma_o h^2$  .

The kinematics of the deformation require that the rates of curvature  $\kappa_r$  and  $\kappa_\phi$  be related to the velocity  $v$  through

$$\kappa_r = -v_{,rr} ; \quad \kappa_\phi = -v_{,r}/r \quad (5)$$

Following the method described in [10] we linearize the constitutive relations by assuming that the stress trajectory in the nine dimensional space of the stress deviator of any particle is a straight line. Thus the quantity  $s_{ij}/(s_{kl}s_{kl})^{1/2} = \text{const.}$  and the stress strain rate relation becomes

$$\epsilon_{ij} = \frac{1}{\tau} (s_{ij} - \bar{s}_{ij})/k \quad (6)$$

where  $\bar{s}_{ij}$  is the state of stress on the surface  $1/2 s_{ij}s_{ij} = k^2$  . This condition is satisfied strictly only at the center of the plate where  $\kappa_r = \kappa_\phi$  and at the edge of the plate where  $\kappa_\phi = 0$  but deviations from the straight line may be small at intermediate points.

The equations relating moments and curvature rates corresponding to (6) are

$$\left. \begin{aligned} \kappa_r &= \frac{\sqrt{3}}{2h\tau} \left( 2M_r - M_\phi - (2\bar{M}_r - \bar{M}_\phi) \right) / M_o \\ \kappa_\phi &= \frac{\sqrt{3}}{2h\tau} \left( 2M_\phi - M_r - (2\bar{M}_\phi - \bar{M}_r) \right) / M_o \end{aligned} \right\} \quad (7)$$

where now  $\bar{M}_r$  and  $\bar{M}_\phi$  are moments satisfying the initial yield condition  $M_r^2 - M_r M_\phi + M_\phi^2 = M_o^2$ .

Using the above relations and Equation (5) the governing equation of the plate velocity  $v$  is

$$\Delta^4 v = \frac{3\sqrt{3}}{4h\tau M_o} \left\{ \frac{1}{r} \left[ (r\bar{M}_r)_{,r} - \bar{M}_\phi \right]_{,r} + p - \mu v_{,t} \right\} \quad (8)$$

The pressure  $p$  in this case is zero except of the region of contact of the plate and the projectile and if the projectile is softer than the plate or vice versa this may be taken as constant over the contact area of radius  $r_o$  and given by

$$\pi r_o^2 p = -Mv_{,t} \Big|_{r=0}$$

where  $M$  is the mass of the projectile.

The quantity

$$-\frac{1}{r} \left[ (r\bar{M}_r)_{,r} - \bar{M}_\phi \right]_{,r}$$

is a pressure distribution and corresponds to that at the static collapse condition of a rigid perfectly plastic plate obeying the von Mises yield condition. We denote the static pressure distribution corresponding to the dynamic loading  $p$  by  $p_o$ . If for example  $p$  is a concentrated point load at  $r = 0$  then  $p_o$  is a concentrated point load of magnitude  $4\pi M_o / \sqrt{3}$ . For other cases

of  $p$  the appropriate  $p_0$  can be obtained by reference to Hopkins and Wang [14].

The problem thus reduces to solving the equation

$$\Delta^4 v + \frac{3\sqrt{3}}{4h\tau M_0} \left( \mu v_{,t} + \frac{M}{\pi r_0^2} v_{,t} \Big|_{r=0} \right) = -p_0 \quad (9)$$

$$0 \leq r < r_0$$

$$\Delta^4 v + \frac{3\sqrt{3}}{4h\tau M_0} \mu v_{,t} = 0 \quad , \quad r_0 < r \leq R$$

subject to an initial specification of  $v$  and to the boundary conditions

$$v(R,t) = 0 \quad , \quad v_{,r}(R,t) = 0 \quad (10)$$

and the regularity conditions

$$\lim_{r \rightarrow 0} v < \infty \quad , \quad \lim_{r \rightarrow 0} v_{,rr} < \infty \quad (11)$$

if the loading is not concentrated, the second of which is modified if it is.

### (iii) General Solution

In developing the subsequent analysis it is convenient to introduce the following dimensionless quantities

$$u = \frac{2h\tau v}{\sqrt{3}R^2} \quad , \quad \rho = \frac{r}{R} \quad , \quad \beta = \frac{M}{\mu R^2} \quad , \quad q_0 = \frac{3p_0 R^2}{2M_0}$$

in terms of which Equation (9) takes the form

$$\left. \begin{aligned} \Delta^4 u + \alpha u_{,t} &= -\alpha \frac{\beta}{\pi \rho_0^2} u_{,t} \Big|_{\rho=0} - q_0 \quad , \quad 0 \leq \rho < \rho_0 \\ &= 0 \quad , \quad \rho_0 < \rho < 1 \end{aligned} \right\} \quad (12)$$

where  $\alpha = \frac{3\sqrt{3}R^4\mu}{4h\tau M_0}$  is a characteristic time of the system and the  $\Delta^4$  represents differentiation with respect to  $\rho$ . The solution of this equation may be written in the form

$$u(\rho, t) = \sum_{n=1}^{\infty} u_n \psi_n(\rho) e^{-\lambda_n^4 \tau / \alpha} - f_0(\rho) \quad (13)$$

where  $\psi_n(\rho)$  is the solution of

$$\left. \begin{aligned} \Delta^4 \psi_n - \lambda_n^4 \psi_n &= \lambda_n^4 \frac{\beta}{\pi \rho_0^2} \psi_n(0) & ; \quad \rho < \rho_0 \\ &= 0 & ; \quad \rho_0 < \rho \end{aligned} \right\} \quad (14)$$

satisfying the boundary conditions  $\psi_n(1) = 0 = \psi_{n,\rho}(1)$  and regularity conditions at  $\rho = 0$  and  $f_0(\rho)$  satisfies

$$\left. \begin{aligned} \Delta^4 f_0 &= q_0 & \rho < \rho_0 \\ &= 0 & \rho_0 < \rho \end{aligned} \right\} \quad (15)$$

and the same conditions at  $\rho = 0$  and 1. The solution for  $\psi_n(\rho)$  takes the form

$$\left. \begin{aligned} \psi_n(\rho) &= A_n^1 J_0(\lambda_n \rho) + A_n^2 Y_0(\lambda_n \rho) + A_n^3 I_0(\lambda_n \rho) \\ &\quad + A_n^4 K_0(\lambda_n \rho), \quad \rho_0 \leq \rho \leq 1, \end{aligned} \right\} \quad (16)$$

and

$$\left. \begin{aligned} \psi_n(\rho) &= A_n^5 J_0(\lambda_n \rho) + A_n^6 I_0(\lambda_n \rho) - \frac{\beta}{\pi \rho_0^2} \psi_n(0), \quad 0 \leq \rho \leq \rho_0. \end{aligned} \right\}$$

The six constants  $A_n^i$  are evaluated in terms of  $\psi_n(0)$  by use of the boundary conditions at  $\rho = 1$  and by continuity of  $\psi_n$  and its derivatives up to the third order at  $\rho = \rho_0$ . Then with  $A_n^5$ ,  $A_n^6$  as linear terms in  $\psi_n(0)$  substitution of  $\rho = 0$  in the second of Equations (16) gives the equation for the eigenvalues  $\lambda_n$ . The indeterminacy of the  $A_n^i$  is removed by setting  $\psi_n(0) = 1$ .

The solution for  $f_0$  takes the form

$$\left. \begin{aligned} f_0(\rho) &= B^1 + B^2 \rho^2 + B^3 \ln \rho + B^4 \rho^2 \ln \rho \\ \text{and} \\ f_0(\rho) &= B^5 + B^6 \rho^2 + q_0 \rho^4 / 64 \end{aligned} \right\} \quad (17)$$

with the constants being determined as above.

In many cases it will be adequate to assume that the radius of the projectile is negligible in comparison with that of the plate in which case  $\rho_0 \rightarrow 0$ . The problem has been examined in [10] and the results obtained there are as follows.

The eigenfunctions  $\psi_n(\rho)$  are

$$\begin{aligned} \psi_n(\rho) &= \frac{1}{2} [J_0(\lambda_n \rho) + I_0(\lambda_n \rho)] - \frac{\lambda_n^2 \beta}{8} \left[ Y_0(\lambda_n \rho) + \frac{2}{\pi} K_0(\lambda_n \rho) \right] \\ &\quad - \frac{\alpha_n}{2} [J_0(\lambda_n \rho) - I_0(\lambda_n \rho)] \end{aligned}$$

where

(18)

$$\alpha_n = \frac{J_0(\lambda_n) + I_0(\lambda_n) - \lambda_n^2 \beta / 4 [Y_0(\lambda_n) + 2/\pi K_0(\lambda_n)]}{J_0(\lambda_n) - I_0(\lambda_n)}$$

and the corresponding eigenvalues  $\lambda_n$  are solutions of the equation

$$\begin{aligned}
 J_0(\lambda_n) I_1(\lambda_n) + J_1(\lambda_n) I_0(\lambda_n) - \frac{\lambda_n^2 \beta}{8} \left\{ \left[ Y_0(\lambda_n) + \frac{2}{\pi} K_0(\lambda_n) \right] [J_1(\lambda_n) + I_1(\lambda_n)] \right. \\
 \left. - \left[ Y_1(\lambda_n) + \frac{2}{\pi} K_1(\lambda_n) \right] [J_0(\lambda_n) - I_0(\lambda_n)] \right\} = 0
 \end{aligned}
 \tag{19}$$

The roots of the eigenvalue equation as functions of  $\beta$  are shown in Fig. 1, including a more expanded scale for the first eigenvalue over the range of interest here.

The eigenfunctions for the case where the mass is concentrated at the point  $\rho_0 = 0$  are orthogonal in the sense that

$$\left. \begin{aligned}
 (\psi_n, \psi_m) &= |\psi_m|^2, & n = m \\
 &= 0, & n \neq m
 \end{aligned} \right\} \tag{20}$$

if we define  $(f, g)$  by

$$(f, g) = 2\pi \int_0^1 \rho f(\rho) g(\rho) d\rho + \beta f(0) g(0) \tag{21}$$

and denote  $(f, f)^{1/2}$  by  $|f|$ .

The initial condition that

$$\left. \begin{aligned}
 u(\rho, 0) &= 0, & \rho \neq 0 \\
 &= u^*, & \rho = 0
 \end{aligned} \right\} \tag{22}$$

where  $u^* = \frac{2h\tau}{\sqrt{3}R^2} V$  with  $V$  the initial velocity of the projectile allows the determination of the  $u_n$  with the resulting solution in the form

$$u(\rho, t) = \sum_{n=1}^{\infty} \left\{ \frac{\beta u^*}{|\psi_n|^2} e^{-\lambda_n^4 t / \alpha} - \frac{(f_0, \psi_n)}{|\psi_n|^2} (1 - e^{-\lambda_n^4 t / \alpha}) \right\} \psi_n(\rho)$$

or alternately

(23)

$$u(\rho, t) = \sum_{n=1}^{\infty} \left\{ \frac{\beta u^* + (f_0, \psi_n)}{|\psi_n|^2} e^{-\lambda_n^4 t / \alpha} \right\} \psi_n(\rho) - f_0(\rho)$$

As is seen from Fig. 1, the first eigenvalue for the values of  $\beta$  covered by the experiments is about 3, the second close to 6 and the third to 9. Since they appear in the form  $\lambda_n^4$  in the exponential term and also in the denominator in the time-wise integrated form of Equation (23) for the deflection it is clear that for any quantities of interest at times away from  $t = 0$  very few terms of the series are needed, and in fact to within estimated accuracy of experimental measurements given in this paper one term only would be adequate.



### III. Experimental and Results

The experimental set up is shown in Fig. 2. The target plates which were 5" diameter were firmly clamped against the ground face of an angular supporting die with a 4" diameter hole leaving a free area of 4" diameter and a 1/2 " deep peripheral region for the clamping action. The whole assembly was bolted to the bed which also supported a rifle with a 0.454" diameter bore. The rifle was aligned so that the projectiles struck the middle of the target area.

The circular target plates, 5" dia. x 0.250" = 0.0005", were made from a C1012 mild steel and used in the as received normalized condition, with hardness Rockwell B 80-81. Two sizes of mild steel (Rockwell B 88-90) cylindrical projectiles were used with masses 31 gm and 10 gm. The dimensions are shown in Fig. 2. The impacting faces of the projectiles had 10" diameter balled ends to enhance interfacial contact between the plate and the projectile during deformation and also to maintain contact should any slight tipping occur during flight.

The velocity of the projectile impact was varied by changing the size of the powder charge according to the calibration curve shown in Fig. 3. This curve was made available by the Stanford Research Institute. The projectile velocity was not measured directly but inferred from the known size of the charge and the calibration curve Fig. 3.

A series of tests were performed in which plates were impacted by two types of projectiles over a range of velocities and the

results are presented in Table 1. The range of velocities was limited at the high end by actual fracturing of the plates, and at the low end the projectiles either fell during the trajectory or there was incomplete burning of the powder due to the smallness of the charge. Only tests in which the projectiles hit the center of the plate were recorded. The profiles of the deformed plates were measured using a transducer and an x-y plotter to obtain the final central deflection,  $\delta$ , which was measured to an accuracy of  $\pm 0.0005$ ". The experimental relationship between the final plate deflection and the energy of the projectile is shown in Fig. 4 for the two projectile masses.

The plastic deformation properties of this C1012 mild steel were determined at two widely different strain-rates to determine the visco-plastic constant. Uniaxial tensile tests were performed at a strain-rate of  $10^{-3} \text{ sec}^{-1}$  and the lower yield stress was determined as 35,000 psi. The lower yield stress was measured at a strain-rate of  $3 \times 10^2 \text{ sec}^{-1}$  using a previously calibrated instrumented Charpy test [15] and was determined as 58,000 psi.

#### IV. Discussion of Results

It is clear from Fig. 4 that the permanent deflection of the plate cannot be related to the energy in a simple manner which is independent of the projectile mass. Replotting the data in terms of momentum produces no better correlation between the results for the different masses. It is of interest to determine whether the general solution presented in Section II, (iii) can produce such a correlation of the data.

Either form of Equation (23) may be used but as it is obvious from Fig. 4. that the method of determining the velocities from the charge size has led to considerable scatter of the results, it is adequate to consider, for times away from  $t = 0$ , an approximate form of the general solution.

To obtain this solution we take only the first term  $n = 1$  and further approximate the first eigenfunction  $\psi_1$  by the function  $f_0(\rho) / f_0(0)$  which we denote by  $\psi_0$ . Equation (23) reduces to the form

$$u(\rho, t) = \left\{ \frac{\beta u^*}{|\psi_0|^2} + f_0(0) \right\} \psi_0(\rho) e^{-\lambda_n^4 t / \alpha} - f_0(\rho) \quad (24)$$

The time  $t_f$  at which the motion stops, given by  $u(\rho, t) = 0$  is

$$t_f = -\frac{\alpha}{\lambda_n^4} \ln \left\{ \frac{f_0(0)}{\frac{\beta u^*}{|\psi_0|^2} + f_0(0)} \right\} \quad (25)$$

and the final deflection  $\delta$  is given by

$$\frac{\delta}{\frac{\sqrt{3} R^2}{2h\tau}} = \int_0^{t_f} u(0,t) dt = \frac{\alpha}{\lambda_1^4} \left\{ \frac{\beta u^*}{|\psi_0|^2} + f_0(0) \ln \left( \frac{f_0(0)}{\frac{\beta u^*}{|\psi_0|^2} + f_0(0)} \right) \right\}$$

In physical quantities this solution takes the form

$$\delta = \frac{3\sqrt{3}}{2\lambda_1^4} \frac{R^4}{h^2\tau^2} \frac{\pi\mu R^2}{P_0} f_0(0) \left\{ \frac{2h\tau}{\sqrt{3} R^2 f_0(0)} V_1 - \ln \left( 1 + \frac{2h\tau}{\sqrt{3} R^2 f_0(0)} V_1 \right) \right\} \quad (26)$$

where  $P_0$  is the static collapse load and  $V_1$  is the initial central velocity in the first mode given by  $V = \beta V / |\psi_0|^2$ . In this result it is clear that the terms dependent on  $\beta$  are  $\lambda_1^4$  and  $V_1$ . Thus if we replot the experimental results as  $\delta\lambda_1^4/h$  versus  $V_1$  we obtain a form of plot in which different values of projectile mass should lie on the same curve. The predicted curve has the form

$$y = \frac{a}{b^2} (bx - \ln(1 + bx))$$

which is quadratic for small  $x$  and asymptotically linear. Determination of the two constants  $a$  and  $b$  allow the determination of the material constants  $P_0$  (and hence  $\sigma_0$ ) and  $\tau$ .

The data given in Table 1 has been replotted in the manner described above and is shown in Fig. 5. It is clear that there is some scatter in the experimental data due largely to the fact the velocities were not directly measured by were inferred the calibration curves Fig. 3. The calibration curves are very steep, particularly for the 10 gm. projectile so that small changes in the charge and

firing conditions can lead to a significant change in the velocity.

In view of the scatter of the experimental points a systematic method for the derivation of constants from the experimental results was not carried out. Instead the results were replotted as already mentioned and predicted curves for reasonable values of  $P_0$  and  $\tau$  were computed and plotted for comparison.

The quantities used in computing the theoretical curves shown in Fig. 5 were as follows. From the previously mentioned instrumented Charpy tests  $\tau$  was taken to be 2.5 msec. From Hopkins and Wang [14] the static collapse load was estimated to be between 10-11  $M_0$ . From other tests we have  $\sigma_0 = 35,000$  psi corresponding to  $P_0$  between 5500 lbs and 6000 lbs. The function  $f_0$  was taken to be

$$f_0(\rho) = \frac{\sqrt{3}}{8} \left[ 1 - \rho^2 (1 - 2 \ln \rho) \right]$$

for which

$$|\psi_0|^2 = 14\pi / 108 + \beta$$

and

$$V_1 = \beta V / (14\pi / 108 + \beta)$$

There is an inconsistency here in that we compute the solution on the basis of a point load for everything except the static yield load  $P_0$ . This is necessary however since the static collapse is very sensitive to the extent of the loaded area around  $\rho_0 = 0$ , as is clear from the fact that it changes from 7.25 at  $\rho = 0$  to about 10 at  $\rho = 0.10$ . The curves obtained from  $P_0 = 5500$  lb and 6000 lb and  $\tau = 2.5$  msec. are shown in Fig. 5 and they are in

good agreement with the results to within the experimental accuracy. A substantial correlation of the data for the two different masses is achieved by this method of plotting the results and thus theory does seem to represent the main features of the response. The theory would however be put to a more severe test if the predictions of the theory regarding the history of the plate velocity and the time needed to bring the projectile to rest could be compared with experimental measurements of these quantities.

## V. Conclusion

An approximate method has been presented for the analysis of a structural model albeit a particularly simple one subjected to a state of dynamic biaxial plastic deformation. The predictions of the theory were compared with experimental results and were found to be in agreement with regard both to the dependence of the final deflection on the impact velocity and the projectile mass.

The general solution obtained here for the clamped circular plate could be extended to other boundary conditions with some increase in the algebraic complexity and could be extended to simply supported rectangular plates. As far as is known no applications to other than plates have been made but many possibilities exist.

In addition to the usefulness of the analytical method the results presented here demonstrate the value of the experimental method as a technique for obtaining dynamic biaxial material characteristics in the plastic range.

### Acknowledgement

The work of the first author was supported by the National Science Foundation under Grant No. GK - 1065 with the University of California, Berkeley. The experimental work was performed through the financial support of the U.S. Army Research Office, Durham, under Contract No. DA31 - 124 ARO (D)251 and the Advanced Research Projects Agency through the Center for Materials Research program at Stanford University.



## References

1. U.S. Lindholm and L.M. Yeakley, "A Dynamic Biaxial Testing Machine", *Experimental Mechanics*, 7, 1, (1967).
2. E.A. Ripperger, "Experimental Studies of Plastic Wave Propagation in Bars", *Plasticity*, E.H. Lee and P.S. Symonds. eds., Pergamon Press, 475, (1960).
3. L.M. Barker, C.D. Lundergan and W. Herrmann, "Dynamic Response of Aluminum", *J. Appl. Phys.*, 35, 1203, (1964).
4. A.J. Wang, "The Permanent Deformation of a Plate Under Blast Loading", *J. Appl. Mech.*, 22, 375, (1955).
5. H.G. Hopkins and W. Prager, "On the Dynamics of Plastic Circular Plates", *Z.A.M.P.*, 5, 317, (1954).
6. A.L. Florence, "Clamped Circular Rigid-Plastic Plates Under Blast Loading", *J. Appl. Mech.*, 33, 256, (1966).
7. A.L. Florence, "Clamped Circular Rigid-Plastic Plates Under Central Blast Loading", *Int. J. Solids Structures*, 2, 319 (1967).
8. A.L. Florence, "Circular Plate Under Uniformly Distributed Impulse", *Int. J. Solids Structures*, 2, 37, (1966).
9. T. Weirzbicki, "Response of Rigid Viscoplastic Circular and Square Plates to Dynamic Loading", *Int. J. Solids Structures*, 3, 635, (1967).
10. J.M. Kelly and T. Weirzbicki, "Motion of a Circular Viscoplastic Plate Subject to Projectile Impact", *Z.A.M.P.*, 18, 236, (1967).
11. P. Perzyna, "The Constitutive Equations for Rate Sensitive Plastic Materials", *Quart. Appl. Math.*, 20, 341, (1963).
12. J.W. Craggs, "A Rate Dependent Theory of Plasticity", *Int. J. Eng. Sci.*, 3, 31, (1965).
13. T. Weirzbicki, "Dynamics of Rigid Viscoplastic Circular Plates", *Arch. Mech. Stos.*, 6, 17, (1965).
14. H.G. Hopkins and A.J. Wang, "Load Carrying Capacity of Circular Plates of Perfectly Plastic Material with Arbitrary Yield Condition", *J. Mech. Phys. Solids*, 3, 117, (1954).
15. C.A. Rau, "Effect of Drilled Holes on Notch Toughness", SUDMS, Rept. 67-12, Stanford University, (1967).

TABLE 1

Plate #	Charge Grains	Mass M gm	Velocity V ft/sec.	Energy $1/2MV^2$ ft.lb	Displacement $\delta$ in $\times 10^{-3}$
1	7	31	670	480	200
5	7	31	670	480	210
6	7	31	670	480	220
40B	8	31	700	500	190
2	10	31	775	640	320
4	10	31	775	640	280
41B	12	31	840	750	350
42B	14	31	960	900	400
7A	5	10	303	30	10
35A	6	10	500	87	25
36A	7	10	750	200	56
42A	7	10	750	200	76
43A	7	10	750	200	64
37A	8	10	960	320	90
44A	8	10	960	320	80
39A	8	10	960	320	80
45A	9	10	1200	500	108
7A	10	10	1504	775	210
47A	11	10	1700	960	184
38A	12	10	1950	1300	220

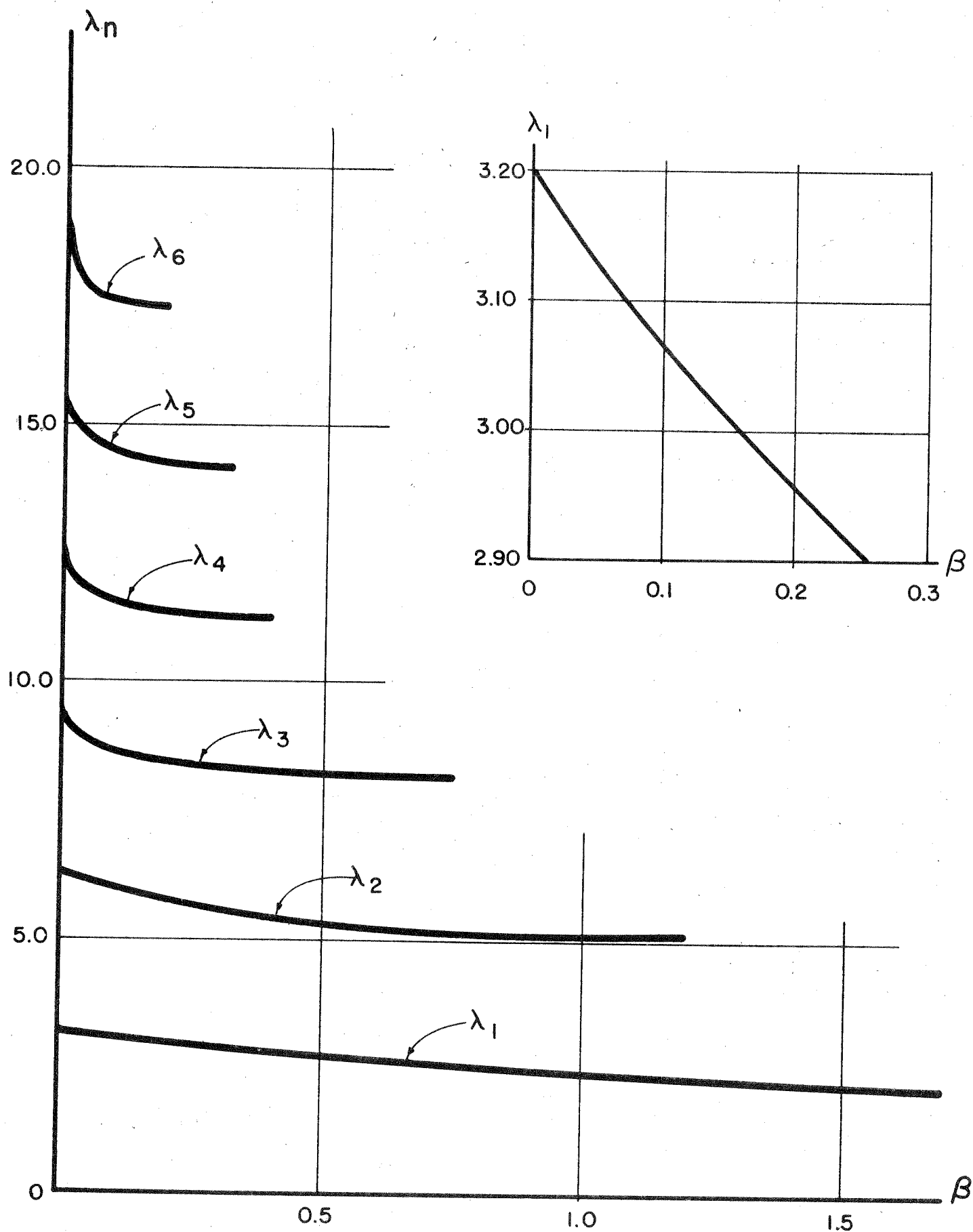


Fig. 1. Eigenvalues as functions of mass ratio  $\beta$ .

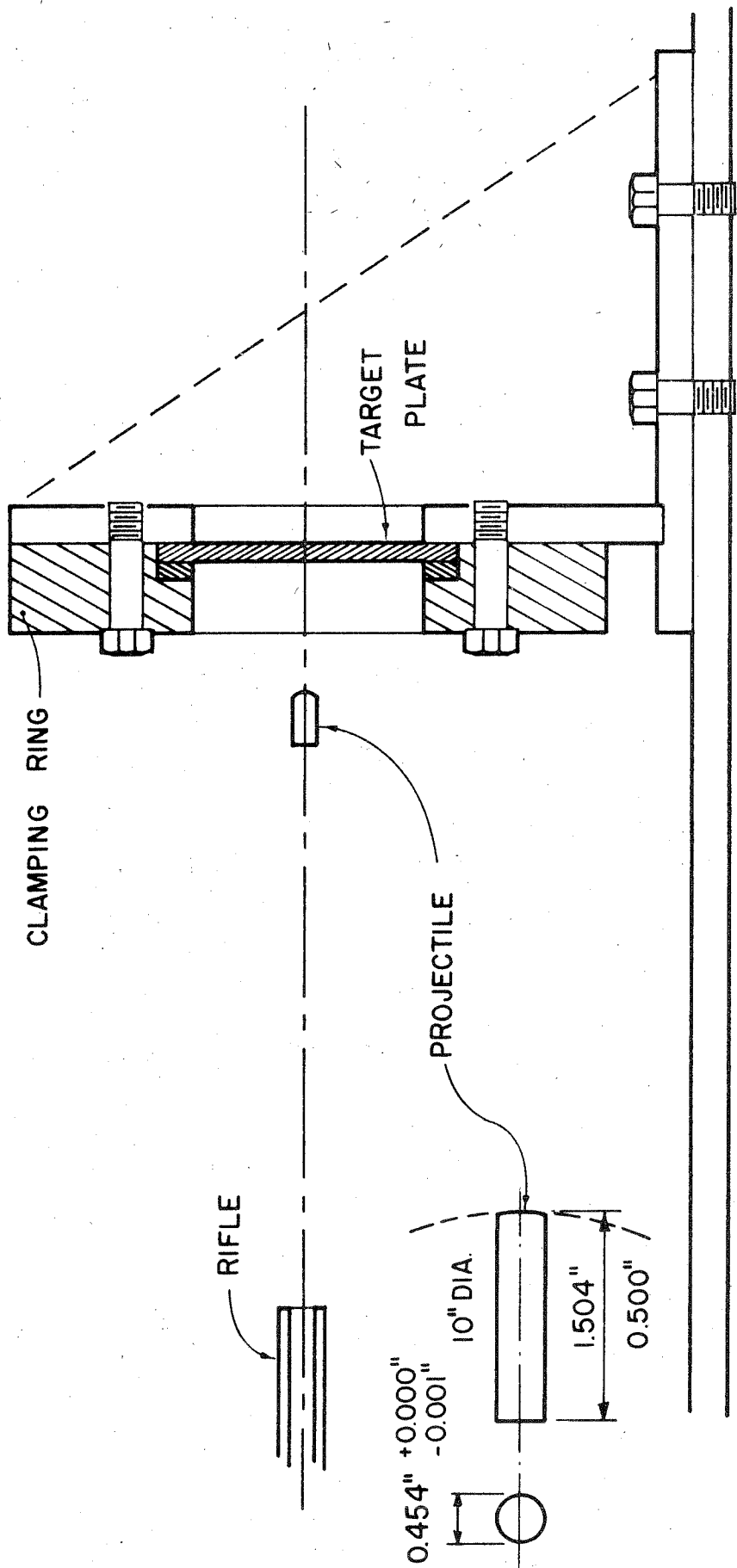


Fig. 2. Diagram of experimental apparatus.

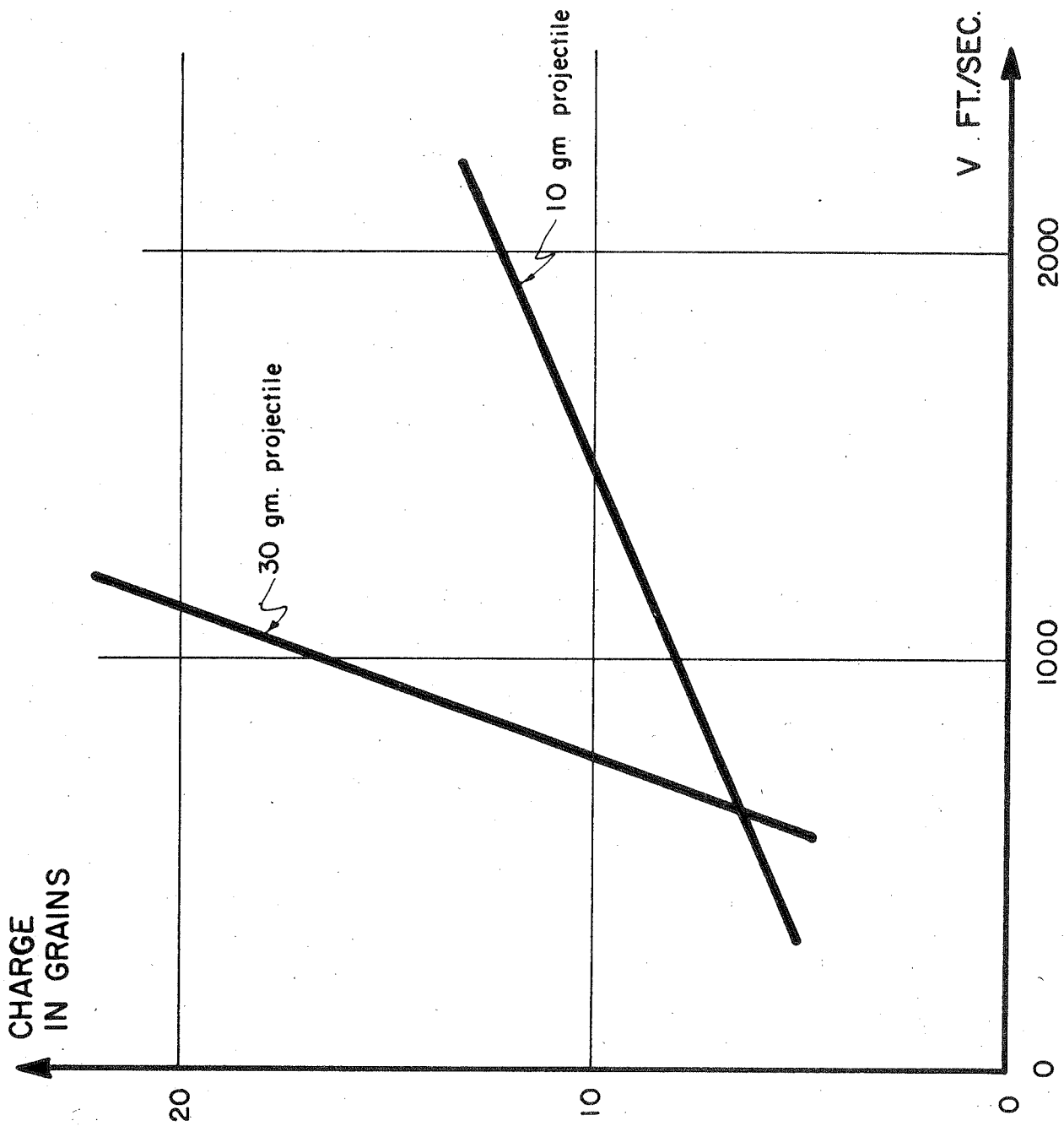


Fig. 3. Calibration curves for velocity in terms of charge size.

This page is left blank

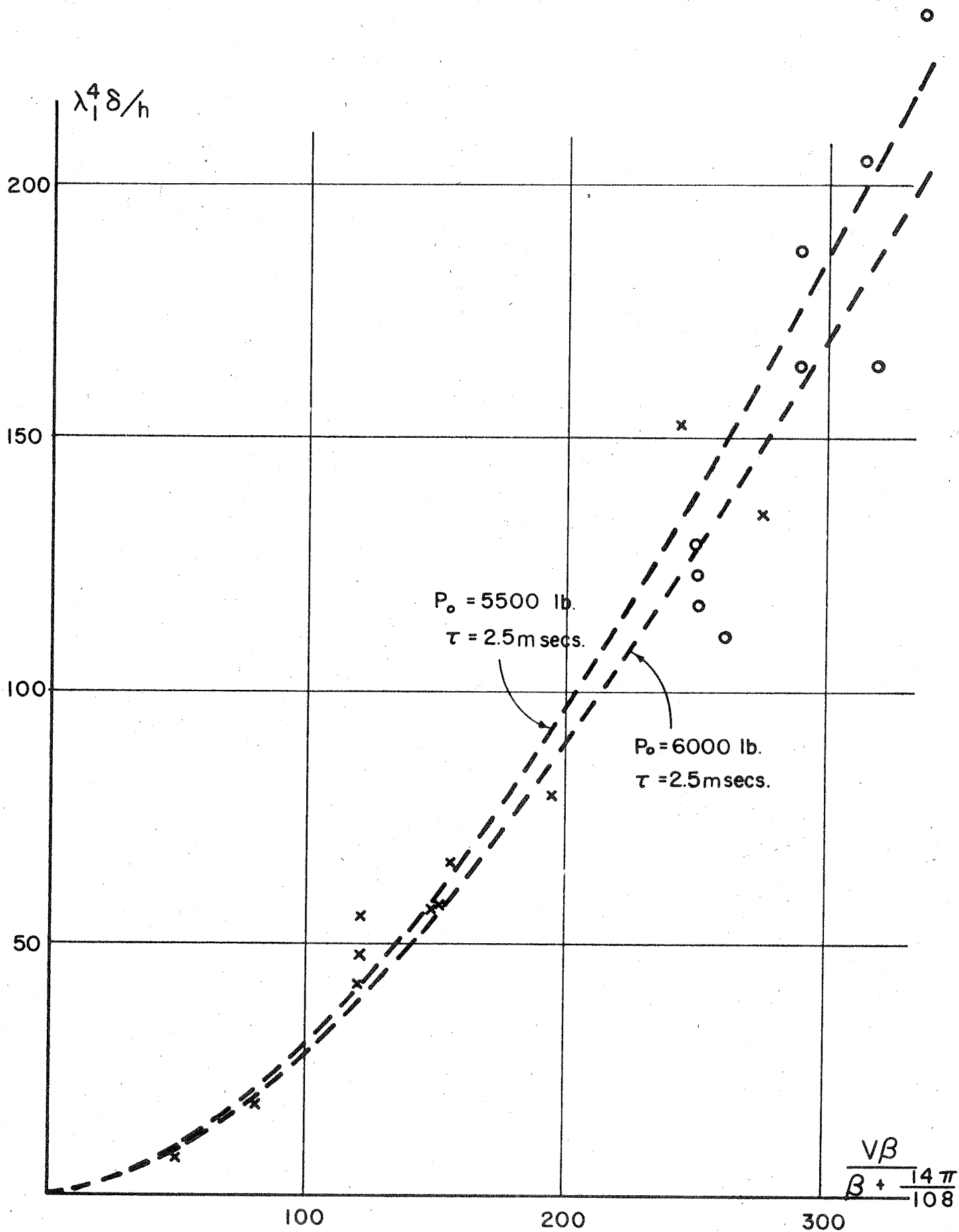


Fig. 5. Correlation of experimental and theoretical results.